NASA Technical Memorandum 106359

An Analysis of Isothermal, Bithermal, and Thermomechanical Fatigue Data of Haynes 188 and B1900+Hf by Energy Considerations

V.M. Radhakrishnan
Indian Institute of Technology
Madras, India

Sreeramesh Kalluri
Sverdrup Technology, Inc.
Lewis Research Center Group
Brook Park, Ohio

and

Gary R. Halford
National Aeronautics and Space Administration
Lewis Research Center
Cleveland, Ohio

September 1993

NASA

AN ANALYSIS OF ISOTHERMAL, BITHERMAL, AND THERMOMECHANICAL FATIGUE DATA OF HAYNES 188 AND B1900+Hf BY ENERGY CONSIDERATIONS

V.M. Radhakrishnan*
Indian Institute of Technology
Metallurgical Engineering Department
Madras, India

Sreeramesh Kalluri
Sverdrup Technology, Inc.
Lewis Research Center Group
Brook Park, Ohio 44142

and

Gary R. Halford
National Aeronautics and Space Administration
Lewis Research Center
Cleveland, Ohio 44135

SUMMARY

The low-cycle fatigue behavior of Haynes 188 and B1900+Hf under isothermal, bithermal, and thermomechanical loading conditions has been analyzed on the basis of the total hysteresis energy expended per cycle. It has been observed that in the case of isothermal fatigue the total hysteresis energy correlates well with the fatigue life. In the case of bithermal "high rate" fatigue, for a given total hysteresis energy per cycle, the fatigue life is equal to or greater than the isothermal fatigue life at the maximum bithermal temperature. This observation could be used to establish a lower bound on life for design purposes. In one case of bithermal creep-fatigue and in thermomechanical fatigue, the life is shorter than that corresponding to the isothermal life at the maximum temperature. The energy supplied, per se, may not always give a systematic correlation with the fatigue life in the cases where time-dependent creep and environmental effects are encountered. Thus, in bithermal creep-fatigue and thermomechanical fatigue, the role of creep and environment and their dependence on the energy supplied have to be properly accounted for before the energy term could be used for life prediction.

INTRODUCTION

Many high-temperature components experience mechanically-imposed cyclic stress and strain during their operation that results in the low-cycle fatigue of the material. Further, during startup or shutdown, the components will be heated or cooled, resulting in thermal gradients and thermal stresses in the material. Thus the thermal stresses-strains, which are superimposed over the cyclic mechanical stresses, will act on the material and may result in additional damage to the component (ref. 1).

Thermomechanical fatigue (TMF), in which material experiences temperature cycling in addition to mechanical stress-strain cycling either in-phase (IP) or out-of-phase (OP) has attracted the attention of

*Previously National Research Council—NASA Senior Research Associate at Lewis Research Center.

many researchers (refs. 2 to 11). TMF loading, which generates closed stress-strain hysteresis loops, introduces a number of damaging mechanisms that are dependent on phasing. During the high-temperature portion in IP loading, creep and relaxation can be introduced in addition to environmental attack, such as oxidation or hot corrosion. Since low temperature is present during compression, healing of small voids generated during creep may not take place. In OP loading, since high temperature is experienced in compression, damage accumulation may not be very severe apart from high temperature environmental attack. However, OP loading will tend to introduce a tensile mean stress (and a high peak tensile stress) which will enhance the damage accumulation rate. Development of tensile mean stress in the OP loading is due to the temperature dependent properties of the material. Tensile mean stress usually has a detrimental effect on fatigue life and such an effect should also be considered in any damage modeling of thermomechanical fatigue.

Bithermal fatigue, in which tension and compression loading regions are kept at constant but different temperatures (T_1 and T_2), has been used by researchers (refs. 2, 3, 9, and 11 to 13) as a first step in understanding the thermomechanical fatigue behavior of materials. During bithermal testing, the specimen is held at near zero stress level while the temperature is changed from T_1 to T_2 (and vice versa) and hence no simultaneous mechanical deformation takes place. Typical hysteresis loops in isothermal, bithermal, and thermomechanical fatigue are shown schematically in figure 1.

The objective of the present study is to investigate whether strain energy density could form a basis for fatigue life analysis in bithermal and thermomechanical loading.

NOMENCLATURE

Cycle types

CC	tensile creep reversed by compressive creep
CCOP	bithermal compressive creep out-of-phase (PC)
CP	tensile creep reversed by compressive plasticity
HRIP	bithermal high rate in-phase (PP)
HROP	bithermal high rate out-of-phase (PP)
IP	in-phase (temperature and mechanical loading)
OP	out-of-phase (temperature and mechanical loading)
PC	tensile plasticity reversed by compressive creep
PP	tensile plasticity reversed by compressive plasticity (pure fatigue)
TCIP	bithermal tensile creep in-phase (CP)
TMIP	thermomechanical in-phase (CP+PP)
TMOP	thermomechanical out-of-phase (PC+PP)

Symbols

E	elastic modulus
E_c	elastic modulus at the temperature where compressive strain reaches a peak in a hysteresis loop
E_t	elastic modulus at the temperature where tensile strain reaches a peak in a hysteresis loop

m	exponent of stress in creep law
N_f	fatigue life in cycles
n	exponent of time in creep law
n'	cyclic strain hardening exponent
P,Q	coefficients of elastic and inelastic energy-fatigue life relations
p,q	exponents of elastic and inelastic energy-fatigue life relations
T	temperature
t	time
t_h	stress-hold time
W_{po}	coefficient of $\delta W_p - \Delta\varepsilon_p$ power-law relation
α	coefficient of thermal expansion
β	exponent of $\Delta\varepsilon_p$ in $\delta W_p - \Delta\varepsilon_p$ power-law relation, $\approx(1 + n')$
$\Delta\varepsilon_{cr}$	time-dependent inelastic (creep) strain range
$\Delta\varepsilon_e$	elastic strain range, $\varepsilon_{e,t} - \varepsilon_{e,c} = (\sigma_t/E_t) - (\sigma_c/E_c)$
$\Delta\varepsilon_p$	time-independent inelastic strain range
$\Delta\varepsilon_t$	total mechanical strain range
$\Delta\sigma$	stress range in a hysteresis loop, $\sigma_t - \sigma_c$
δW_c	time-dependent inelastic strain energy density
δW_e	elastic strain energy density
δW_p	time-independent inelastic strain energy density
$\delta W_{p,c}$	compressive time-independent inelastic strain energy density
$\delta W_{p,t}$	tensile time-independent inelastic strain energy density
δW_t	total strain energy density, $\delta W_e + \delta W_p$
ε_{elong}	elongation in a tensile test
$\varepsilon_{e,c}$	elastic strain at peak compressive strain in a hysteresis loop
$\varepsilon_{e,t}$	elastic strain at peak tensile strain in a hysteresis loop
ε_T	total mechanical and thermal strain
ε_t	total mechanical strain
ε_{th}	thermal strain
σ_c	stress at peak compressive strain in a hysteresis loop
σ_{cr}	stress at which a hold is introduced in tension or compression
σ_t	stress at peak tensile strain in a hysteresis loop
σ_y	0.2-percent offset yield strength

ENERGY CONSIDERATION IN LOW-CYCLE FATIGUE

Basic Parameters in Fatigue Analysis

There are a number of basic parameters employed in the analysis of high-temperature, low-cycle fatigue. They are mostly based on the strain range (refs. 3, 5, and 10),—either inelastic or total strain range—in which the time-dependent effects are introduced through functions of frequency, strain rate, tension- or compression-going times, or creep strain. Stress range occasionally is also used to describe the fatigue life of materials. Some models are based on the inelastic strain energy density (i.e., hysteresis energy) and have been successfully applied to predict the low-cycle fatigue life of materials (refs. 14 to 21). Energy-based approaches consider both imposed stress and strain and hence may be a better representation of the actual fatigue conditions experienced by materials. Consider, for example, the comparative fatigue lives of Haynes 188 at 927 °C and B1900+Hf at 871 °C, as shown in figure 2, based on both inelastic strain range and stress range. The temperatures are close enough to make a reasonable comparison. Haynes 188 shows a greater fatigue life based on inelastic strain range, but not so based on stress range. This is mainly because Haynes 188 is more ductile, but weaker than B1900+Hf. Thus both ductility and strength dictate whether a material is superior to another when inelastic strain or stress is taken as the parameter. To avoid possible ambiguity, both stress- and strain-parameters are required to analyze the fatigue life. This is accomplished commonly by using total strain range, which is a sum of both the elastic (stress range/elastic modulus) and inelastic strain ranges, as shown in figure 3. An alternative method of combining stress and strain to analyze fatigue life is to use strain energy density as a parameter.

Isothermal Low-Cycle Fatigue

In high-frequency, low-cycle fatigue, where the time-independent effects are dominant (PP-type loading), the total strain energy density supplied to the material can be divided into elastic strain energy density, δW_e, and time-independent inelastic strain energy density, δW_p. The elastic strain energy density in a hysteresis loop (fig. 4) can be defined by the relation

$$\delta W_e = \int_{\varepsilon_{e,c}}^{\varepsilon_{e,t}} \left(\sigma \, d\varepsilon_e\right) = \left(\frac{\Delta\sigma \, \Delta\varepsilon_e}{2}\right) \tag{1}$$

Note that equation (1) does not represent the elastic strain energy density at any given instant of loading in a cycle. It actually represents the elastic strain energy density in a given hysteresis loop. The time-independent inelastic strain energy density, δW_p, represented by the area of the hysteresis loop, can be given in the form (refs. 14 and 15)

$$\delta W_p = \oint \left(\sigma \, d\varepsilon_p\right) = \left(\frac{1 - n'}{1 + n'}\right) \Delta\sigma \, \Delta\varepsilon_p \tag{2}$$

where $(1 - n')/(1 + n')$ usually is between 0.6 and 0.8. The schematic hysteresis loops shown in figure 4 have the same elastic and time-independent inelastic strain energy densities despite different mean stresses. This is because these loops have identical stress and total strain ranges. Such an invariance of

cyclic stress-strain curve at different levels of mean stress was experimentally observed by Manson and Halford (ref. 22).

In the case of a stress-hold, a time-dependent creep strain range, $\Delta\varepsilon_{cr}$, will be introduced and the strain energy density associated with the hold time, t_h, is defined by

$$\delta W_c = |\sigma_{cr}| \int_0^{t_h} |\dot{\varepsilon}_{cr}| \, dt = |\sigma_{cr}| \, \Delta\varepsilon_{cr} \tag{3}$$

where $|\sigma_{cr}|$ corresponds to the magnitude of the stress at which hold is introduced and $\dot{\varepsilon}_{cr}$ is the creep rate. During this hold period, damage is caused by time-dependent phenomena such as creep, environmental effects, and metallurgical changes in the material (refs. 23 and 24).

The above method of energy computation has been extended to bithermal fatigue by considering each portion of the hysteresis in tension and compression separately.

Bithermal Fatigue

In the case of high-rate bithermal fatigue (HRIP and HROP), where the time-dependent effects will be negligible, the tensile and compressive portions of loading are at different temperatures. The hysteresis energies in tensile and compressive portions of the cycle can be obtained from equation (2) by replacing $\Delta\sigma$ with the magnitudes of the stresses at peak tensile and compressive strains (σ_t and $|\sigma_c|$), respectively, as

$$\delta W_{p,t} = \left(\frac{1 - n'}{1 + n'}\right) \sigma_t \, \Delta\varepsilon_p \tag{4}$$

and

$$\delta W_{p,c} = \left(\frac{1 - n'}{1 + n'}\right) |\sigma_c| \, \Delta\varepsilon_p \tag{5}$$

where the cyclic strain hardening exponent n' could be a function of temperature and in equations (4) and (5) values of n' corresponding to the temperatures in the tensile and compressive portions of the cycle should be used.

In the case of stress-hold either in tension or in compression (TCIP and CCOP), the energy associated with creep deformation can be computed using equation (3) and that of the plastic deformation using equation (4) or (5) depending on the type of rapid loading (tension or compression).

Thermomechanical Fatigue

Thermomechanical fatigue (TMIP and TMOP), where mechanical straining and temperature variation take place simultaneously, is difficult to analyze because material properties like ductility, strain hardening exponent, modulus, yield strength, etc., are continuously changing with temperature. Typical variation of stress and strain in a TMOP fatigue test is shown in figure 5 for Haynes 188. In TMOP loading the mechanically imposed strain decreases along with an increase in the temperature. Depending on the compressive going time, creep and relaxation effects will take place. This will decrease the compressive stress developed as the compressive strain increases. However, the value of the peak compressive stress developed in the hysteresis loop will depend on the strain hardening nature of the material at the different imposed temperatures.

In thermomechanical loading, the total strain in the material is a combination of elastic, plastic, creep, and thermal strains. Thus we have

$$\varepsilon_T = \varepsilon_e + \varepsilon_p + \varepsilon_{cr} + \varepsilon_{th} \tag{6}$$

The thermal strain, ε_{th}, is given in terms of the temperature range, ΔT and the coefficient of thermal expansion, α as

$$\varepsilon_{th} = \alpha \, \Delta T \tag{7}$$

Thus we have the resultant mechanical strain rate equation

$$\dot{\varepsilon}_t = \dot{\varepsilon}_e + \dot{\varepsilon}_p + \dot{\varepsilon}_{cr} = \dot{\varepsilon}_T - \alpha \dot{T} \tag{8}$$

The dot above each variable denotes the corresponding time rate of change. $\dot{\varepsilon}_t$ is the imposed mechanical strain rate which may remain constant in a given strain rate controlled test. The elastic strain rate is given by

$$\dot{\varepsilon}_e = \frac{\dot{\sigma}}{E} \tag{9}$$

The time-independent inelastic (plastic) strain can be expressed in terms of the 0.2-percent offset yield strength, σ_y and n' as

$$\varepsilon_p = 0.002 \left(\frac{\sigma}{\sigma_y} \right)^{(1/n')} \tag{10}$$

From Equation (10) the time-independent inelastic (plastic) strain rate is obtained as

$$\dot{\varepsilon}_p = \frac{0.002}{n' \sigma_y} \left(\frac{\sigma}{\sigma_y} \right)^{[(1-n')/n']} \dot{\sigma} \tag{11}$$

By assuming a creep law

$$\varepsilon_{cr} = A\,\sigma^{m}\,t^{n} \tag{12}$$

the creep strain rate is obtained as

$$\dot{\varepsilon}_{cr} = nA^{1/n}\sigma^{m/n}\varepsilon_{cr}^{[(n-1)/n]} + m\varepsilon_{cr}\left(\frac{\dot{\sigma}}{\sigma}\right) \tag{13}$$

In general, the constants α, E, σ_y, n', A, m, and n in the above equations are temperature dependent.

By substituting equations (9), (11), and (13) in equation (8) and solving equation (8), stress can be obtained as a function of time or strain. The energy computation can be carried out by a numerical method taking small increments of stress or strain.

DATA ANALYSIS

Database

The fatigue data for the present analysis of Haynes 188 and B1900+Hf have been taken from reference 2. Typical variation of the tensile elongation for the two materials is shown in figure 6 (ref. 2). Haynes 188 shows high ductility, whereas B1900+Hf has low ductility. In the case of Haynes 188, isothermal, low-cycle fatigue test results had been reported for 316, 704, 760, and 927 °C. No isothermal creep-fatigue results were reported in reference 2. In- and out-of-phase bithermal and thermomechanical fatigue tests were conducted between 316 and 760 °C. In bithermal tests both fatigue and creep-fatigue types of loading modes were used. The cycle duration in thermomechanical tests was 3 min. In the case of B1900+Hf isothermal, bithermal, and thermomechanical fatigue tests were conducted at and between 483 and 871 °C. In bithermal and thermomechanical fatigue only the out-of-phase loading mode was employed. The cycle duration in thermomechanical tests was 4 min.

Hourglass specimens were used in the investigation and measured diametrical displacements were subsequently converted to axial strains.

Isothermal Fatigue Results

The following power-law equations are used to represent relationships between elastic and inelastic strain energy densities and fatigue life.

$$\delta W_e = P(N_f)^{p} \tag{14}$$

$$\delta W_p = Q(N_f)^{q} \tag{15}$$

The constants in equations (14) and (15) are obtained with life as the dependent variable. The relationship between total strain energy density, δW_t and fatigue life, N_f can be obtained by the addition of

equations (14) and (15). However, for a majority of fatigue life prediction purposes such a relationship essentially contains the same information as that in equations (14) and (15). Therefore, in the rest of the raper, these simpler life relationships are used.

The relations between the elastic and the time-independent inelastic strain energy densities per cycle and the number of cycles to failure at the four temperatures of testing, are shown in figures 7(a) and (b) for Haynes 188. The relations log (δW_p) versus log (N_f) yield straight lines parallel to each other in the temperature range investigated indicating that a common exponent of -0.77 can be used to fit the relations between the time-independent inelastic strain energy density and the fatigue life. Similarly, a common exponent of -0.2 is used to fit the relations between the elastic strain energy density and fatigue life. The constants for all the life relations are listed in table I.

Figure 7(c) shows the relations between the time-independent inelastic energy absorbed and the fatigue life for B1900+Hf. The variation of elastic strain energy density with life is also shown in the figure and it can be seen that the transition life where the elastic energy is equal to the inelastic energy, is very low in the case of B1900+Hf at 871 °C, i.e., around 25 cycles compared to 1300 and 2500 cycles, respectively, at 760 and 316 °C for Haynes 188. This is because B1900+Hf has significantly lower ductility and higher strength than Haynes 188. The life relation constants for B1900+Hf are also given in table I.

Since inelastic strain range governs low-cycle fatigue life and inelastic strain energy density is used to characterize the fatigue life in this paper, it is worthwhile to examine how these two quantities are related for the alloys investigated. The relation between the inelastic strain energy density and the inelastic strain range is given by the power-law equation

$$\delta W_p = W_{po}(\Delta\varepsilon_p)^{\beta} \tag{16}$$

where δW_p is in Nmm/mm^3, $\beta \approx 1 + n'$, and

$$W_{po} \approx \left(\frac{1 - n'}{1 + n'}\right)\left(\frac{2^{(1-n')}\sigma_y}{(0.002)^{n'}}\right) \tag{17}$$

The $\delta W_p - \Delta\varepsilon_p$ plot clearly demonstrates a one-to-one correspondence between the inelastic strain range and the inelastic strain energy density in a hysteresis loop. For Haynes 188 such a relation, under isothermal loading at 316 and 760 °C, is shown in figure 8(a). The data yield a straight line on the log-log plot with a slope nearly equal to $(1 + n')$.

Figure 8(b) shows the relation between δW_p and $\Delta\varepsilon_p$ for B1900+Hf at 483 and 871 °C. The constants W_{po} and β (obtained with inelastic strain range as the independent variable), and implied values of cyclic strain hardening exponent n' at these selected temperatures for Haynes 188 and B1900+Hf are listed in table II.

Bithermal Fatigue Results

Energy expended in bithermal fatigue.—The total inelastic strain energy density (δW_p) in a hysteresis loop is a sum of the tensile ($\delta W_{p,t}$) and compressive ($\delta W_{p,c}$) portions of the inelastic strain energy densities. In the case of an isothermal fatigue test inelastic strain energy densities in the tensile half of the

hysteresis loop and the compressive half of the hysteresis loop are equal and each value represents one-half of the total inelastic strain energy density in the hysteresis loop i.e., $\delta W_{p,t} = \delta W_{p,c} = \delta W_p/2$. However, in a bithermal fatigue test $\delta W_{p,t}$ is likely to be different from $\delta W_{p,c}$ due to different temperatures in tensile and compressive halves of the hysteresis loop. It is worthwhile to compare the inelastic strain energy densities observed in the bithermal tests to those observed in the isothermal fatigue tests. Such a comparison, when performed at a given inelastic strain range for the entire hysteresis loop and for the tensile and compressive halves of the hysteresis loop, provides the similarities and differences in the inelastic energies expended in isothermal and bithermal fatigue tests.

(a) Haynes 188

Figures 9(a) and (b) show the relation between the time-independent inelastic strain energy density and the inelastic strain range in the case of HRIP and HROP type of tests for Haynes 188. Note that at any given strain range, the inelastic strain energy associated with the half cycle at 316 or 760 °C ($\delta W_{p,t}$ or $\delta W_{p,c}$) in bithermal fatigue is marginally higher than the corresponding energy in a isothermal half cycle ($\delta W_p/2$) during fatigue. Likewise, at a given inelastic strain range, the total inelastic strain energy density (sum of the tensile and compressive portions of the inelastic strain energy densities, $\delta W_{p,t} + \delta W_{p,c}$) in bithermal fatigue is slightly larger than that observed in isothermal fatigue (δW_p). A further comparison of the inelastic strain energy densities in HRIP and HROP tests shown in figures 9(a) and (b), indicates that in both cases the inelastic strain energy absorbed at a given inelastic strain range is nearly the same. The relation between the inelastic energy density and the inelastic strain range for the bithermal tests can also be described by equation (16). The constants W_{po} and β for these tests are listed in table II. The inelastic strain energy in the compressive half of the TCIP cycle ($\delta W_{p,c}$) and the inelastic strain energy in the tensile half of the CCOP cycle ($\delta W_{p,t}$) are also shown in figures 9(a) and (b), respectively. In both cases, the half-cycle inelastic energy in bithermal creep-fatigue is marginally higher than the corresponding isothermal half-cycle inelastic energy ($\delta W_p/2$).

(b) B1900+Hf

Figure 9(c) shows the relation between time-independent inelastic strain energy density absorbed and the inelastic strain range in tension (483 °C) and compression (871 °C) for the HROP fatigue tests. The inelastic energy associated with the tensile or compressive halves ($\delta W_p/2$) of isothermal fatigue cycles at these two temperatures are also shown in the figure. The inelastic energy in the tensile half of the CCOP cycle ($\delta W_{p,t}$) is also shown in the figure. It can be seen that there is negligible difference between the inelastic energy absorbed in the tension portion of the out-of-phase loading in bithermal fatigue, whether the compression portion is in time-independent inelastic (plasticity) or time-dependent inelastic (creep) type of deformation. As discussed before, equation (16) can be used to describe the relation between δW_p and $\Delta\epsilon_p$ for HROP tests. The constants W_{po} and β are tabulated in table II for B1900+Hf.

Life relations in bithermal fatigue.—

(a) Haynes 188

Figures 10(a) and (b) show the relations between inelastic strain energy expended and fatigue life for bithermal fatigue and creep-fatigue tests, respectively. The solid lines are for isothermal tests at 316 and 760 °C (see fig. 7(a)). HRIP test results fall on the isothermal line corresponding to 760 °C. The HROP results fall on a line displaced from, but parallel to and between, the isothermal lines. For a given total inelastic strain energy density the in-phase fatigue life is less than the out-of-phase fatigue life as was the case for inelastic strain range versus cyclic life (ref. 2). However, it can be noted that the isothermal fatigue life at the maximum temperature, namely, 760 °C, can be used as a lower bound for rapid loading bither-

mal fatigue in the studied temperature regime. For fatigue lives less than 2000 cycles, TCIP loading is more damaging than its counterpart HRIP loading (fig. 10(b)). In general, when compared on the basis of inelastic strain energy density, the in-phase lives are less than the out-of-phase lives. Further, note that for any fatigue life less than 2000 cycles, TCIP life is lower than the isothermal life at the maximum temperature. Hence for Haynes 188 the isothermal inelastic energy density life relation at the maximum temperature cannot be used as a lower bound in the case of bithermal creep-fatigue especially at low-cyclic lives for in-phase loading.

The life relations between the elastic strain energy and the bithermal fatigue life are shown in figures 10(c) and (d) for fatigue and creep-fatigue type of tests. The solid lines denote the trends of isothermal tests at 316 and 760 °C. HRIP and HROP test results are bounded by the isothermal lines with the HROP data near the 316 °C isothermal line (fig. 10(c)). Even on the basis of elastic strain energy density, HRIP fatigue lives are lower than the HROP fatigue lives. The TCIP and CCOP fatigue lives are lower than the high rate isothermal fatigue lives at 760 °C, which indicates that for bithermal creep-fatigue, the elastic strain energy density life relation obtained at the maximum temperature cannot be used as a lower bound for life estimation.

(b) B1900+Hf

Figures 11(a) and (b) show the $\delta W_p - N_f$ and $\delta W_e - N_f$ relations for B1900+Hf for out-of-phase bithermal fatigue and creep-fatigue. The isothermal relations are also given corresponding to the maximum temperature namely, 871 °C. In general, with the exception of one datum, for both cases the fatigue lives are higher than those of the isothermal condition. Hence, for B1900+Hf between 483 and 871 °C and for fatigue lives less than 2000 cycles, the isothermal fatigue life relation corresponding to the maximum temperature could be taken as the lower bound for design purposes. The constants for all bithermal fatigue life relations are given in table I.

Thermomechanical Fatigue

In thermomechanical fatigue the temperature changes continuously with the applied strain in a cycle which causes a variation in the material properties such as the elastic modulus and the cyclic strain hardening exponent. For example, the cyclic strain hardening exponent n′ of Haynes 188 varies between 0.14 and 0.17 in the temperature range of 316 and 760 °C (ref. 2). Likewise, for B1900+Hf, n′ varies between 0.094 and 0.30 in the temperature range of 483 and 871 °C (ref. 2). The inelastic strain energy densities associated with the tensile and compressive portions of a TMF cycle for Haynes 188 and B1900+Hf have been computed with equations (4) and (5) by assigning a value of 0.16 (see table II) for the cyclic strain hardening exponent. The values of stresses corresponding to the peak tensile and compressive mechanical strains have been used for σ_t and σ_c. Such a computation yields an approximate value of the inelastic strain energy density which is actually given by the area in a TMF hysteresis loop. The tensile and compressive elastic strain energy densities have been computed approximately by using equation (1). Accurate computation of the elastic strain energy density can be obtained by using increments of stress and strain.

The inelastic strain energy density versus life and the elastic energy density versus life for Haynes 188 and B1900+Hf are shown in figures 12(a) and (b). In general, the TMIP and TMOP fatigue lives of Haynes 188, when compared on the basis of inelastic strain energy density, cluster near the isothermal life line corresponding to 760 °C (fig. 12(a)). At high δW_p values two TMIP tests and at a low δW_p value one TMOP test have cyclic lives that are lower than the corresponding isothermal lives at maximum temperature. This clearly indicates that the inelastic strain energy density versus fatigue life relation at

the maximum isothermal temperature can not be used as a lower bound for estimating thermomechanical fatigue lives of Haynes 188 between 316 and 760 °C. However, when compared on the basis of elastic strain energy density, the TMIP and TMOP cyclic lives are higher than the corresponding lives at the maximum isothermal temperature (fig. 12(a)). At higher elastic and inelastic strain energy densities, for Haynes 188, TMIP has lower lives than TMOP and the opposite is true at lower values of energy densities. The TMOP lives of B1900+Hf are lower than the corresponding fatigue lives at the maximum isothermal temperature especially at lower energy densities (fig. 12(b)). The observed low-fatigue lives of Haynes 188 and B1900+Hf under TMOP loading at smaller values of strain energy densities are possibly due to the tensile mean stresses generated in the TMOP hysteresis loops. Tensile mean stress usually has a detrimental effect on fatigue life and the magnitude of this detrimental effect increases with decreasing inelastic strain range (or inelastic strain energy density) (ref. 25). The life relationship constants for TMF tests are listed in table I.

DISCUSSION

An energy based approach holds the promise of being a viable fatigue life prediction methodology as it combines the stress and strain ranges. It is able to adequately correlate the isothermal fatigue lives for the available data on Haynes 188 and B1900+Hf. Its accuracy is as good as that of the strain range parameter (ref. 2), because the inelastic strain energy density and the inelastic strain range can be related by equations (16) and (17). If fatigue life relations can be established for a material with elastic and inelastic strain ranges, then fatigue life relations also exist for that material on the basis of elastic and inelastic strain energy densities because the energy densities and the strain ranges are related. However, the strain energy density as such may not be able to give a good correlation with fatigue life in bithermal and thermomechanical fatigue. For example, in the case of HRIP and HROP tests on Haynes 188, for the same inelastic strain range, and thus for the same inelastic strain energy density (eq. (16)), the fatigue life in HRIP is lower than that in HROP (fig. 9(a)). Further, introduction of hold time in bithermal fatigue and thermomechanical fatigue can produce different fatigue lives for the same energy input. For most materials tensile loading at high temperature is usually more damaging than compressive loading at high temperature. Under in-phase loading, stress assisted oxidation, hot corrosion, and creep play a part in enhancing the damage accumulation at any given energy level. Thus, while evaluating the damage parameter based on energy, the effects of time-dependent damage factors such as oxidation, hot corrosion, and their interaction with creep damage should be properly taken into account for a rational analysis and reliable prediction of low-cycle fatigue life. The energy term, per se, will not be able to give a correlation with the fatigue life in bithermal or thermomechanical fatigue where time-dependent effects enhance the damage accumulation.

The relations between the total strain range, $\Delta\varepsilon_t$, and the fatigue life, N_f, for all fatigue test data used in this investigation are shown in figures 13(a) and (b) for the two materials. In these figures, factors of 2 on fatigue life, at 760 °C for Haynes 188 and at 871 °C for B1900+Hf, are shown by the dashed lines. It can be observed that in-phase tests in bithermal fatigue with hold time and in TMF give lower fatigue lives than the high rate isothermal fatigue (PP) tests at the maximum temperature, 760 °C, in the case of Haynes 188. Other types of tests in bithermal and thermomechanical fatigue have fatigue lives that are either equal to or greater than the high rate isothermal fatigue (PP) tests at 760 °C. Thus for practical design purposes, the Haynes 188 life relation ($\Delta\varepsilon_t - N_f$) at 760 °C can be used in the fatigue life regime investigated for all types of loading other than in-phase type where oxidation and creep effects in tension at high temperature also contribute to damage. With the data available for B1900+Hf it can be seen that TMOP loading is more severe than the isothermal testing at the maximum temperature. At lower strain ranges it can be seen that the reduction in fatigue life is rather pronounced. The out-of-phase mode introduces a tensile mean stress (and a high peak tensile stress) which will be more detrimental to fatigue life. However, the detrimental effect of tensile mean stress on fatigue life tends to diminish as the

inelastic strain range increases in the hysteresis loop (ref. 25). In bithermal and thermomechanical fatigue, for life evaluation of low-ductility materials with energy as a parameter, the elastic energy density should be considered in addition to inelastic time-independent and time-dependent energy densities.

CONCLUDING REMARKS

From the analysis carried out on the isothermal, bithermal, and thermomechanical fatigue data of Haynes 188 and B1900+Hf the following conclusions are drawn.

1. The elastic and inelastic strain energy densities can be used to characterize the isothermal, bithermal, and thermomechanical low-cycle fatigue behaviors of Haynes 188 and B1900+Hf. The governing life relations are expressed as power-laws in terms of fatigue life and the corresponding strain energy densities.

2. In isothermal fatigue tests of Haynes 188 and B1900+Hf, the inelastic strain energy density can be related to the inelastic strain range by a power-law relation. The exponent of inelastic strain range in such a relation is directly related to the cyclic strain hardening exponent of the material at that temperature.

3. In bithermal fatigue of Haynes 188, both in HRIP and HROP tests, the sum of the tensile and compressive portions of the inelastic strain energy densities is marginally higher than the sum of the individual isothermal components at the temperatures 316 and 760 °C at any given value of the inelastic strain range. However, the difference is not very significant. This difference in energy level between isothermal and bithermal loading is also observed in the case of B1900+Hf. Even in bithermal fatigue tests of Haynes 188 and B1900+Hf the inelastic strain energy density can be related to the total inelastic strain range by a power-law.

4. For the same energy input, HRIP loading has lower fatigue life than HROP loading in Haynes 188. Likewise, the TCIP loading also has lower life than CCOP loading for Haynes 188. In general, for the same energy level in-phase loading is more detrimental than out-of-phase loading for Haynes 188.

5. For the same energy level, bithermal out-of-phase loading in B1900+Hf in both rapid loading and stress-hold conditions, has higher fatigue life than the corresponding isothermal fatigue life at the maximum temperature.

6. In general, for the same energy input, thermomechanical fatigue in both the materials results in lower life than the isothermal fatigue at the maximum temperature.

7. Energy based approach is able to adequately correlate isothermal, high loading rate, low-cycle fatigue data. However, in bithermal and thermomechanical fatigue where the time-dependent effects of environment and creep enhance the damage accumulation, energy per se is not sufficient to predict the fatigue life under different conditions of loading even though it can be used to characterize the fatigue life for a specific loading condition. Any damage parameter with energy as the basis must also account for the effects of oxidation and creep under creep-fatigue and nonisothermal conditions.

ACKNOWLEDGMENT

One of the authors (VMR) is thankful to National Research Council, Washington, DC, for their financial help.

REFERENCES

1. Halford, G.R., Low Cycle Thermal Fatigue, Thermal Stresses II, R.B. Hetnarski, Ed., Elsevier Science Publishers, B.V. Amsterdam, 1987, pp. 330–428.

2. Halford, G.R., Verrilli, M.J., Kalluri, S., Ritzert, F.J., Duckert, R.E., and Holland, F.A., Thermomechanical and Bithermal Fatigue Behavior of Cast B1900+Hf and Wrought Haynes 188, Advances in Fatigue Life Time Predictive Techniques, ASTM STP–1122, M.R. Mitchell and R.W. Landgraf, (Eds.), ASTM, Philadelphia, 1992, pp. 120–142.

3. Halford, G.R., McGaw, M.A., Bill, R.C., and Fanti, P.D., Bithermal Fatigue: A Link Between Isothermal and Thermomechanical Fatigue, Low Cycle Fatigue, ASTM STP–942, H.D. Solomon, G.R. Halford, L.R. Kaisand, and B.N. Leis, (Eds.), ASTM, Philadelphia, 1988, pp. 625–637.

4. Marchand, N., L'Esperance, G., and Pelloux, R.M., Thermal-Mechanical Cyclic Stress-Strain Responses of Cast B-1900+Hf, ibid., 1988, pp. 638–656.

5. Malpertu, J.L. and Remy, L., Thermomechanical Fatigue Behavior of a Superalloy, ibid., 1988, pp. 657–671.

6. Holmes, J.W., McClintock, F.A., O'Hara, K.S., and Conners, M.E., Thermal Fatigue Testing of Coated Monocrystalline Superalloys, ibid., 1988, pp. 672–691.

7. Cook, T.S., Kim, K.S., and McKnight, R.L., Thermal-Mechanical Fatigue of Cast Rene 80, ibid., 1988, pp. 692–708.

8. Bill, R.C., Verrilli, M.J., McGaw, M.A., and Halford, G.R., A Preliminary Study of the Thermomechanical Fatigue of Polycrystalline MAR M–200, NASA TP–2280, AVSCOM TR 83–C–6, 1984.

9. Sheffler, K.D., Vacuum Thermal-Mechanical Fatigue Testing of Two Iron Base High Temperature Alloys, NASA CR–134524, 1974.

10. Halford, G.R. and Manson, S.S., Life Prediction of Thermal-Mechanical Fatigue Using Strain Range Partitioning, Thermal Fatigue of Materials and Components, ASTM STP–612, D.A. Spera and D.F. Mowbray, (Eds.), ASTM, Philadelphia, 1973, pp. 473–481.

11. Lindholm, U.S. and Davidson, D.L., Low Cycle Fatigue with Combined Thermal and Strain Cycling, Fatigue at Elevated Temperature, ASTM STP–520, A.E. Carden, A.J. McEvily and C.H. Wells, (Eds.), ASTM, Philadelphia, 1972, pp. 473–481.

12. McDowell, D.L., and Miller, M.P., Physically Based Microcrack Propagation Laws for Creep-Fatigue-Environment Interaction, Creep-Fatigue Interaction at High Temperature, ASME AD–Vol.21, G.K. Haritos and O.O. Ochoa, Eds., 1991, pp. 19–30.

13. Müller, T. and Gerold, V., Isothermal and Bithermal Fatigue of a Directionally Solidified Ni-Based Superalloy, Scripta Metallurigica et Materialia, Vol. 26, 1992, pp. 1343–1348.

14. Morrow, J., Cyclic Plastic Strain Energy and Fatigue of Metals, Internal Friction, Damping, and Cyclic Plasticity, ASTM STP–378, American Society for Testing and Materials, 1965, pp. 45–84.

15. Halford, G.R., The Energy Required for Fatigue, Journal of Materials, Vol. 1, No. 1, 1966, pp. 3–18.

16. Ostergren, W.J., Correlation of Hold Time Effects in Elevated Temperature Low Cycle Fatigue Using a Frequency Modified Damage Function, 1976 ASME–MPC Symposium on Creep-Fatigue Interaction, 1976, pp. 179–202.

17. Leis, B.N., An Energy-Based Fatigue and Creep-Fatigue Damage Parameter, Transactions of the ASME, Journal of Pressure Vessel Technology, 1977, pp. 524–533.

18. Radhakrishnan, V.M., An Analysis of Low Cycle Fatigue Based on Hysteresis Energy, Fatigue of Engg. Mater. Struct., 3(1), 1980, pp. 75–82.

19. Radhakrishnan, V.M., Life Prediction in Time Dependent Fatigue, Proc. Inter. Conf. on Advances in Life Prediction Methods, D.A. Woodford and J.R. Whitehead (Eds.), ASME, 1983, pp. 143–150.

20. He, J., Duan, Z., Ning, Y., and Zhao, D., Strain Energy Partitioning and Its Application to GH33A Nickel Base Superalloy and 1Cr18Ni9Ti Stainless Steel, ibid., 1983, pp. 27–32.

21. Ellyin, F. and Asada, Y., Time-Dependent Fatigue Failure: The Creep-Fatigue Interaction, Int. J. Fatigue, 13, No. 2, 1991, pp. 157–164.

22. Manson, S.S. and Halford, G.R., Correction: Practical Implementation of the Double Linear Damage Rule and Damage Curve Approach for Treating Cumulative Fatigue Damage, International Journal of Fracture, Vol. 17. No. 4, Aug. 1981, pp. R35–R42.

23. Kalluri, S., Generalization of The Strainrange Partitioning Method for Predicting High Temperature Low Cycle Fatigue Life at Different Exposure Times, Ph.D. Thesis, Dept. of Mech. and Aerospace Eng., Case Western Reserve University, Cleveland, OH, 1987.

24. Agatonovic, P. and Taylor, N., Optimization of a Life Prediction Method for Environmentally Assisted Damage Components Operating at High Temperature, Proc. Mechanical Behavior of Materials, ICM–6, M. Jono and T. Inoue, (Eds.), Vol. 2, 1991, pp. 303–310.

25. Halford, G.R. and Nachtigall, A.J., Strainrange Partitioning Behavior of an Advanced Gas Turbine Disk Alloy AF2–1DA, AIAA 79–1192R, Journal of Aircraft, Vol. 17, No. 8, 1980, pp. 598–604.

TABLE I.—Constants for Energy-Fatigue Life Relations (eqs. (14) and (15))

Material	Test Type	Temperature* (°C)	P (Nmm/mm^3)	p	Q (Nmm/mm^3)	q
Haynes 188	Isothermal	316	19	−0.2	5000	−0.77
"	"	704	16	"	1300	"
"	"	760	13	"	600	"
"	"	927	4.8	"	750	"
"	HRIP	760 <-> 316	13	−0.18	600	"
"	HROP	316 <-> 760	18	−0.22	1100	"
"	TCIP	760 <-> 316	5	−0.11	110	−0.56
"	CCOP	316 <-> 760	"	"	300	−0.67
"	TMIP	760 <-> 316	10	−0.13	250	−0.54
"	TMOP	316 <-> 760	66	−0.44	235500	−1.77
B1900+Hf	Isothermal	483	20	−0.17	120	−0.74
"	"	871	25	−0.32	140	−0.84
"	HROP	483 <->871	88	−0.46	3500	−1.25
"	CCOP	"	20	−0.24	190	−0.71
"	TMOP	"	65	−0.42	470	−1.14

*In bithermal and TMF tests, the first value denotes temperature in tension and at the tensile peak strain, respectively. Likewise, the second value denotes temperature in compression and at the compressive peak strain in bithermal and TMF tests.

TABLE II.—Constants for $\delta W_p - \Delta\varepsilon_p$ Relation (eq. (16))

Material	Test Type	Temperature* (°C)	W_{po} (Nmm/mm^3)	β	$\beta - 1$ ($\approx n'$)
Haynes 188	Isothermal	316	1850	1.16	0.16
"	"	760	"	"	"
"	HRIP	760 <-> 316	2300	"	"
"	HROP	316 <-> 760	"	"	"
B1900+Hf	Isothermal	483	2850	1.10	0.10
"	"	871	2750	1.22	0.22
"	HROP	483 <-> 871	2930	1.16	0.16

*In bithermal fatigue tests, the first value denotes the temperature in tension and the second value denotes the temperature in compression.

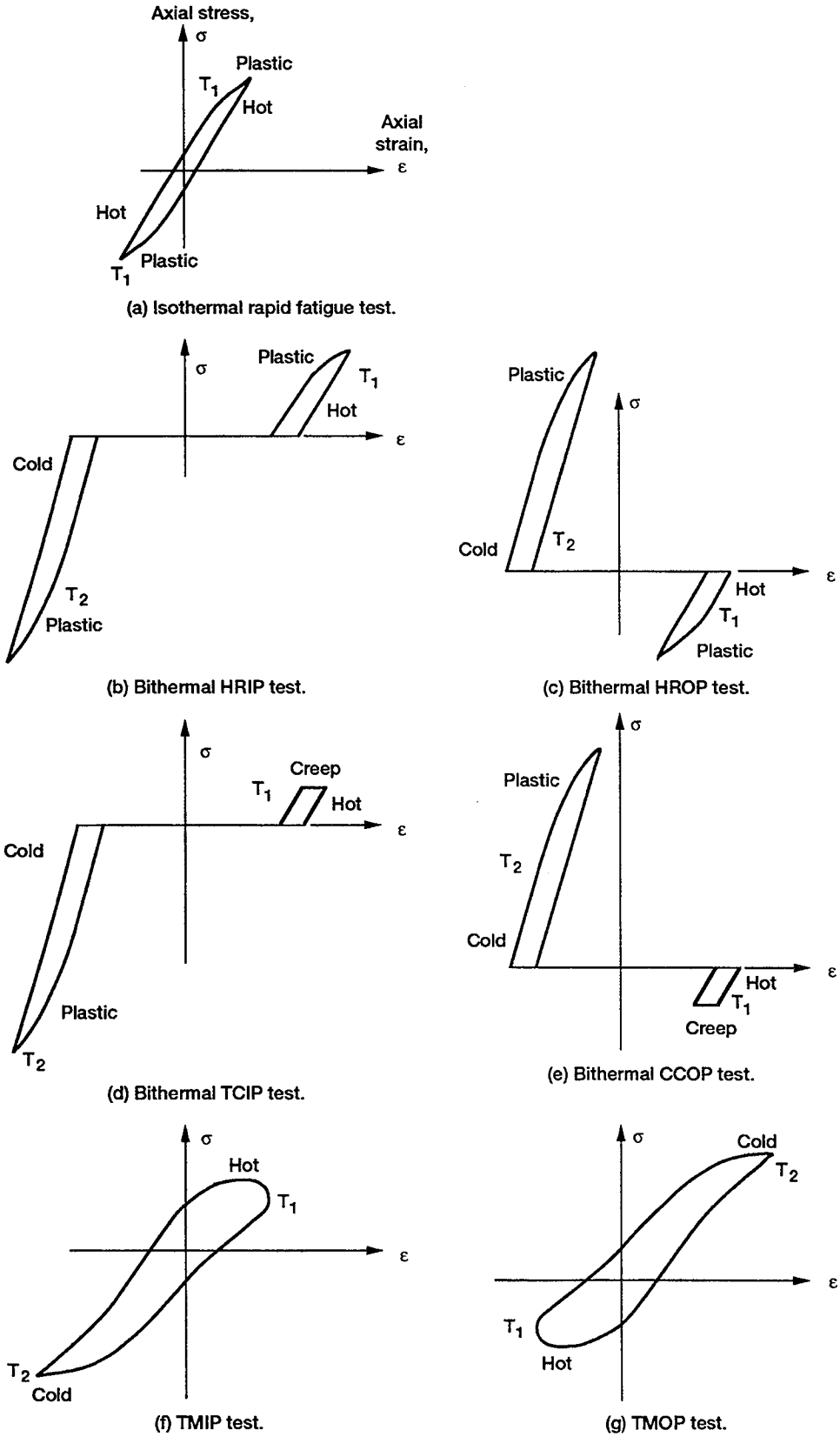

Figure 1.—Schematic representation of hysteresis loops in isothermal, bithermal, and thermomechanical fatigue, $T_1 > T_2$.

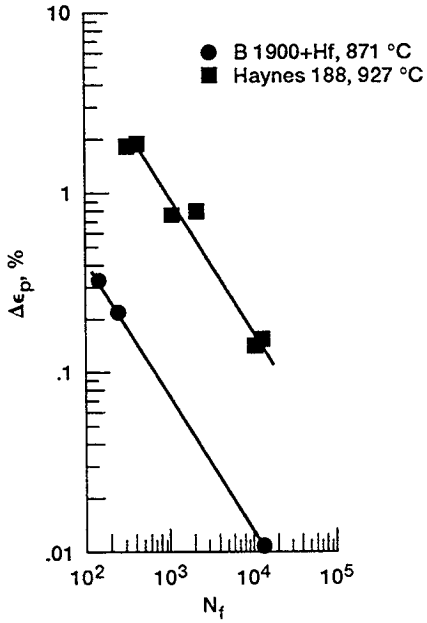

(a) $\Delta\epsilon_p$-N_f relations.

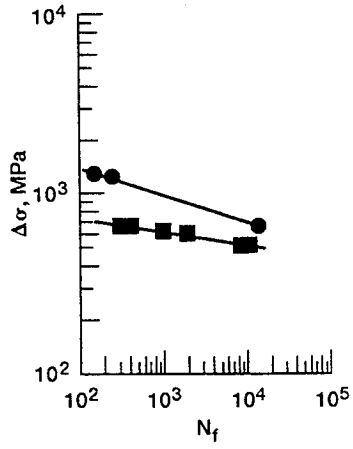

(b) $\Delta\sigma$-N_f relations.

Figure 2.—Comparison of isothermal fatigue life based on inelastic strain range and stress range for Haynes 188 and B1900+Hf.

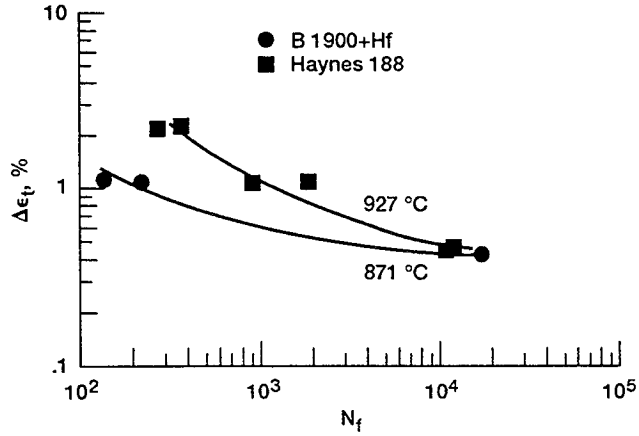

Figure 3.—Comparison of fatigue life based on total strain range.

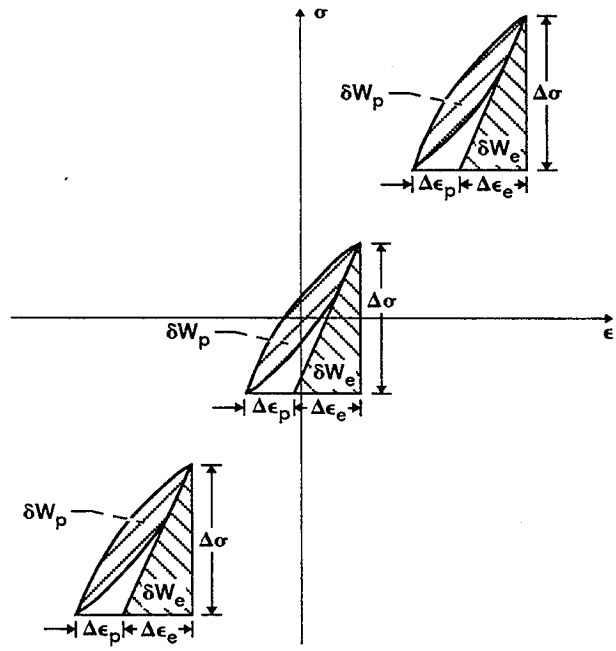

Figure 4.—Schematic illustration of elastic and time-independent inelastic strain energy densities in hysteresis loops.

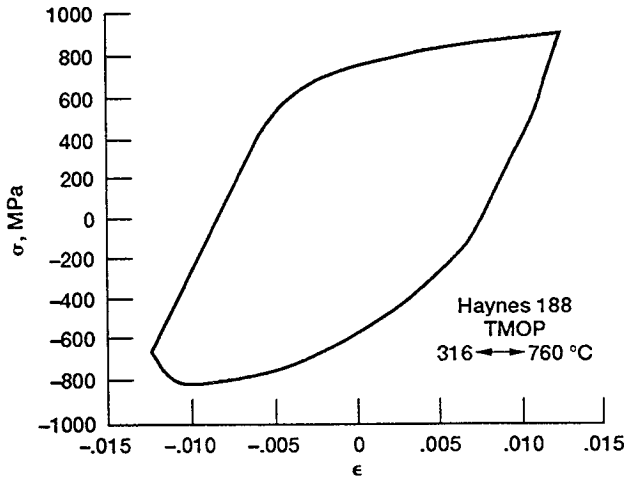

Figure 5.—Typical hysteresis loop in an out-of-phase thermomechanical fatigue test.

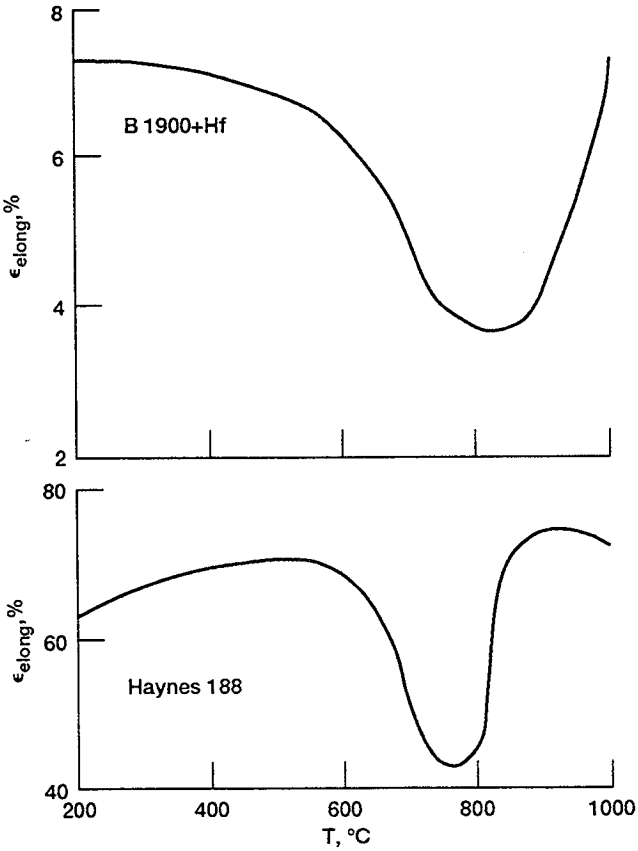

Figure 6.—Variation of tensile elongation with temperature for Haynes 188 and B1900+Hf.

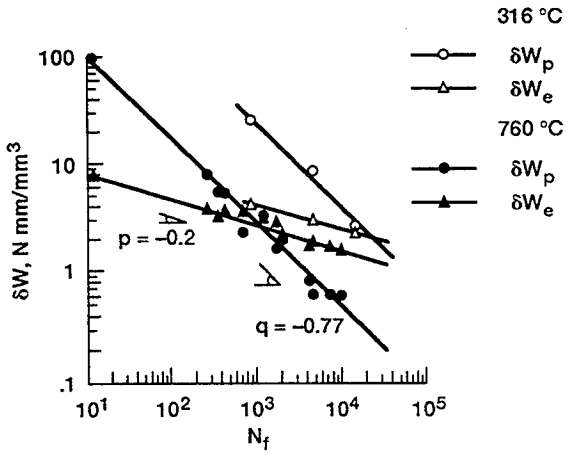

(a) Haynes 188 at 316 and 760 °C.

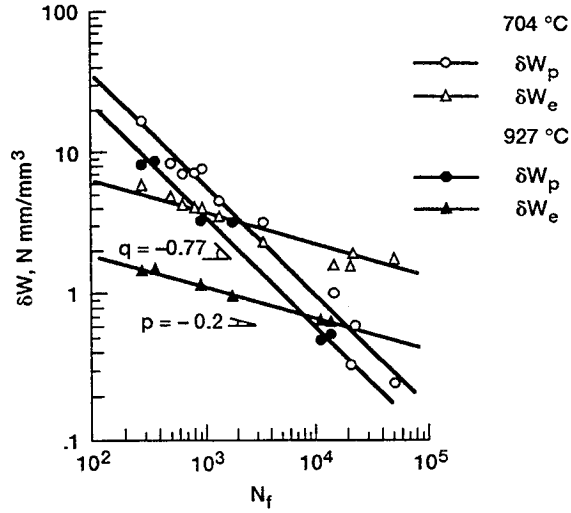

(b) Haynes 188 at 704 and 927 °C.

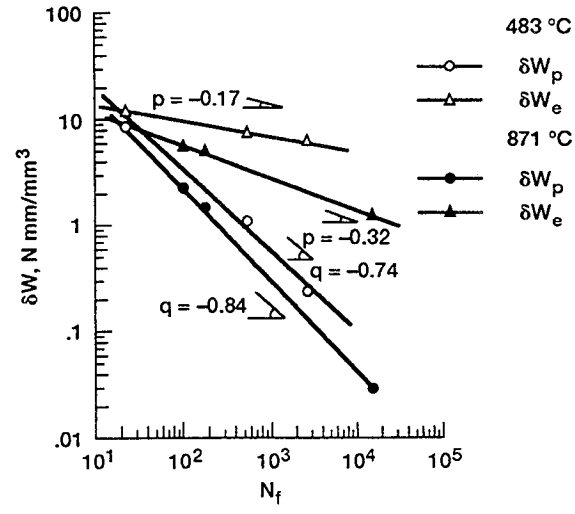

(c) B1900+Hf at 483 and 871 °C.

Figure 7.—Relations between strain energy density per cycle and fatigue life in isothermal tests.

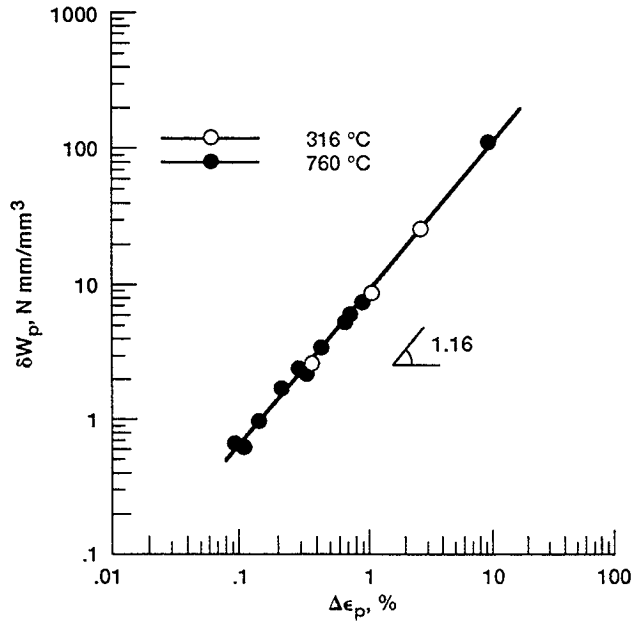

(a) Haynes 188 at 316 and 760 °C.

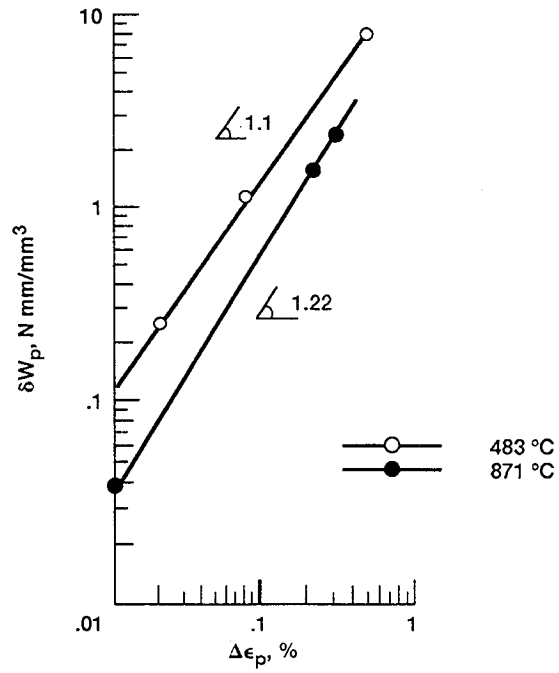

(b) B1900+Hf at 483 and 871 °C.

Figure 8.—Relations between time-independent inelastic strain energy density and inelastic strain range in rapid isothermal fatigue.

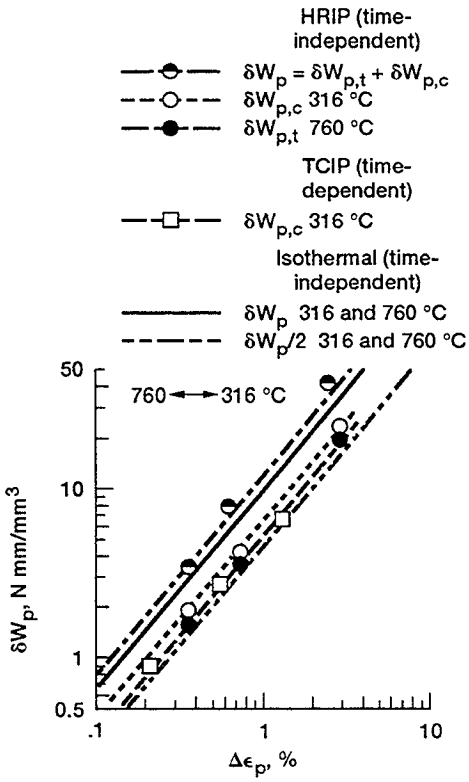

(a) Haynes 188, HRIP and TCIP tests.

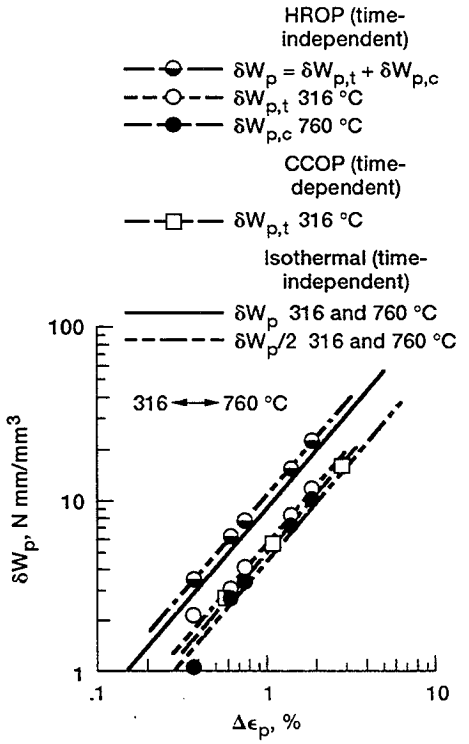

(b) Haynes 188, HROP and CCOP tests.

Figure 9.—Relations between time-independent inelastic strain energy density and inelastic strain range in bithermal fatigue.

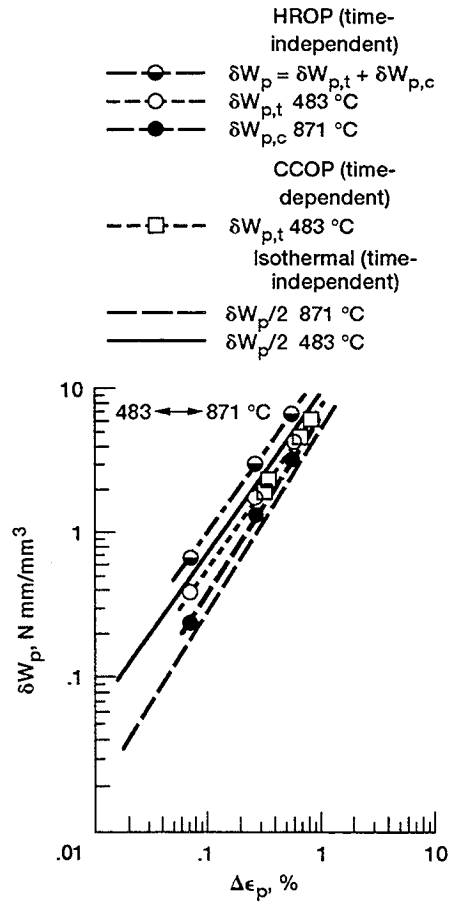

(c) B1900+Hf, HROP and CCOP tests.

Figure 9.—Concluded.

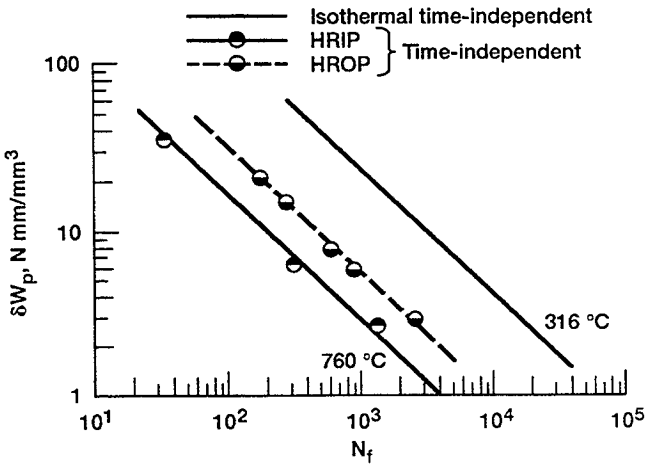

(a) δW_p-N_f for HRIP and HROP tests.

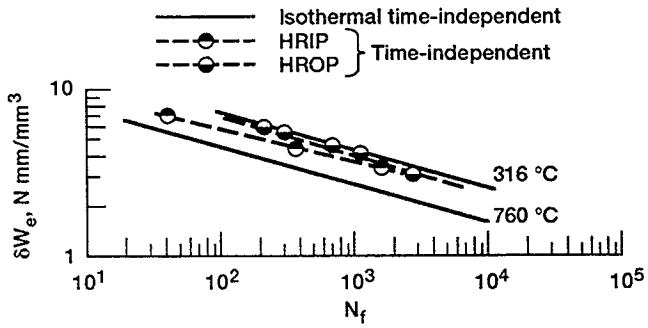

(c) δW_e-N_f for HRIP and HROP tests.

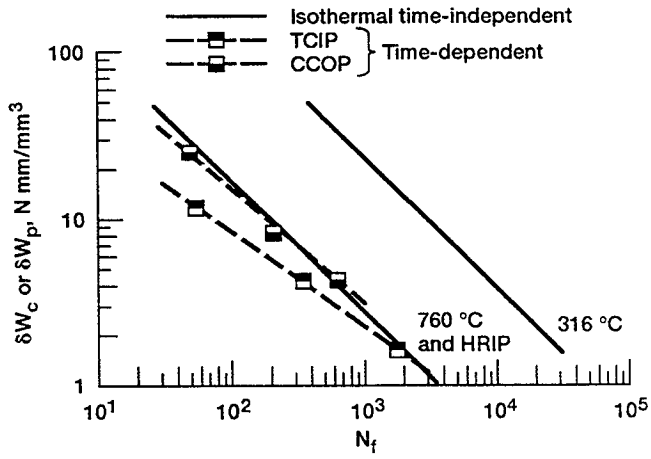

(b) δW_c-N_f for TCIP and CCOP tests.

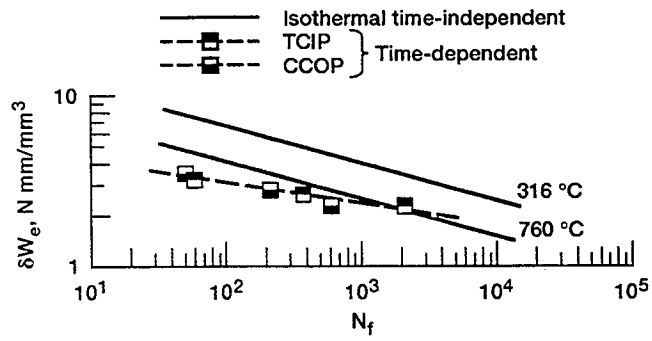

(d) δW_e-N_f for TCIP and CCOP tests.

Figure 10.—Relations between strain energy density and fatigue life for Haynes 188 in bithermal fatigue and creep-fatigue.

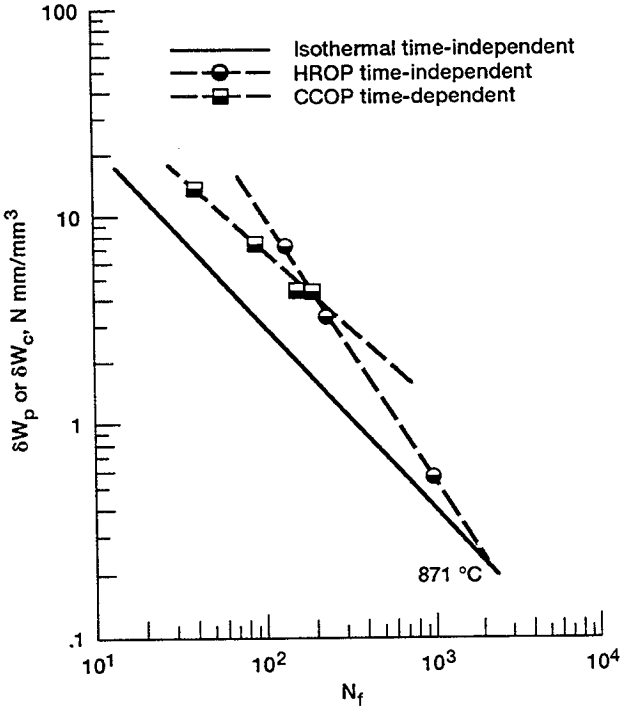

(a) δW_p-N_f for HROP and δW_c-N_f for COOP test.

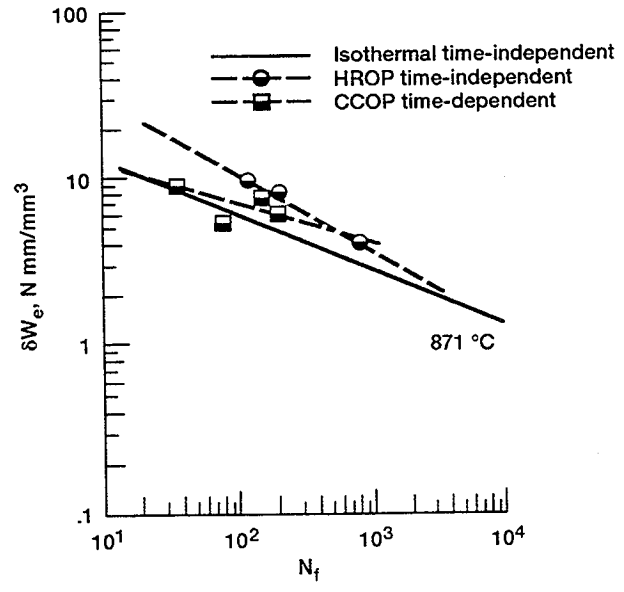

(b) δW_e-N_f for HROP and COOP test.

Figure 11.—Relations between strain energy density and fatigue life in bithermal fatigue of B1900+Hf.

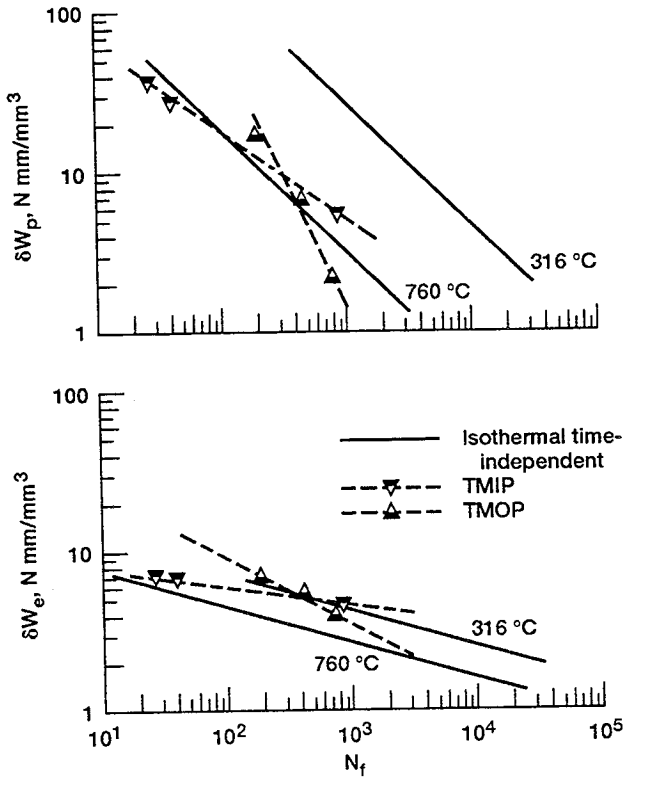

(a) Haynes 188.

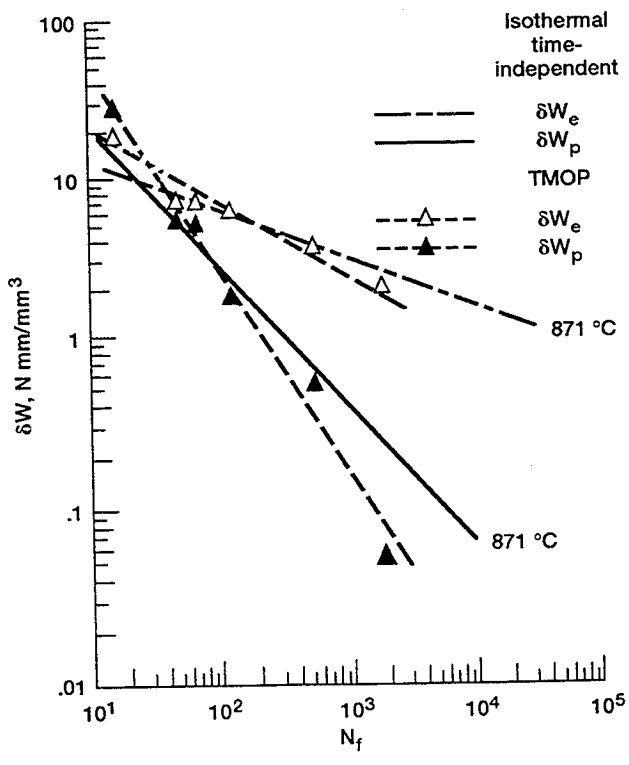

(b) B1900+Hf.

Figure 12.—Relations between inelastic strain energy density and fatigue life and elastic strain energy density and fatigue life for thermomechanical fatigue tests.

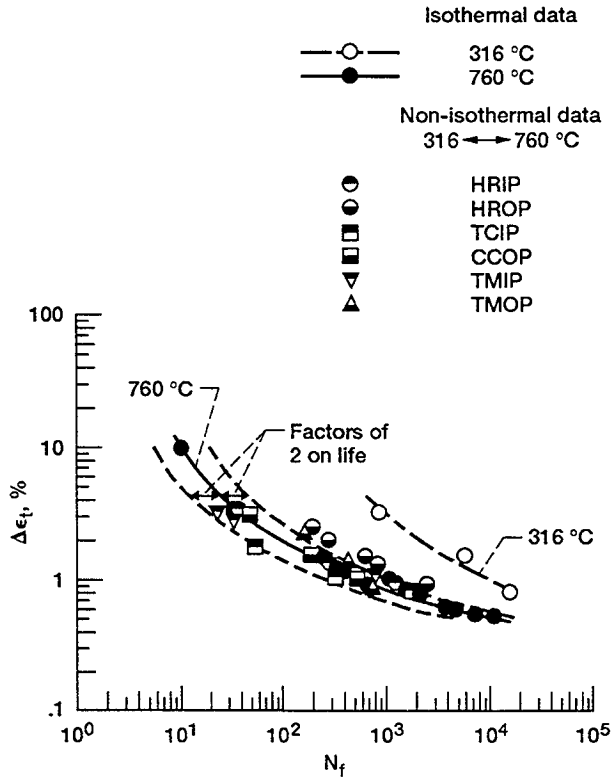

(a) Haynes 188.

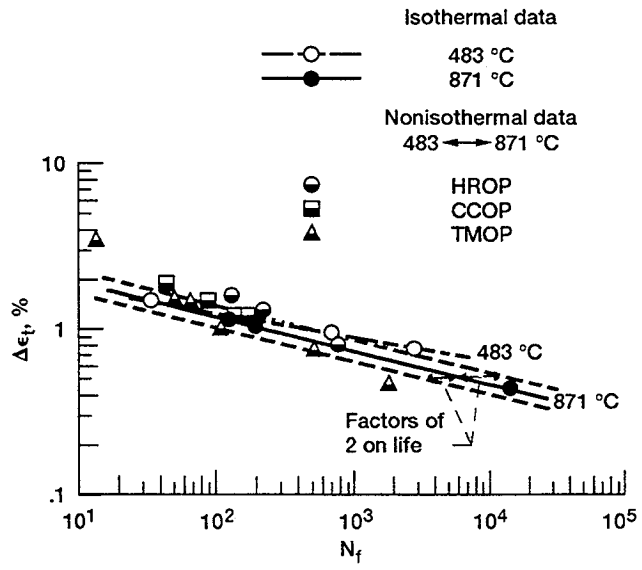

(b) B1900+Hf.

Figure 13.—Relations between total strain range and fatigue life for all types of loading. Solid line is for isothermal life at the maximum temperature.

REPORT DOCUMENTATION PAGE

Form Approved
OMB No. 0704-0188

1. AGENCY USE ONLY (*Leave blank*)	2. REPORT DATE	3. REPORT TYPE AND DATES COVERED
	September 1993	Technical Memorandum

4. TITLE AND SUBTITLE

An Analysis of Isothermal, Bithermal, and Thermomechanical Fatigue Data of Haynes 188 and B1900+Hf by Energy Considerations

5. FUNDING NUMBERS

WU-505-63-5B

6. AUTHOR(S)

V.M. Radhakrishnan, Sreeramesh Kalluri, and Gary R. Halford

7. PERFORMING ORGANIZATION NAME(S) AND ADDRESS(ES)

National Aeronautics and Space Administration
Lewis Research Center
Cleveland, Ohio 44135-3191

8. PERFORMING ORGANIZATION REPORT NUMBER

E-8153

9. SPONSORING/MONITORING AGENCY NAME(S) AND ADDRESS(ES)

National Aeronautics and Space Administration
Washington, D.C. 20546-0001

10. SPONSORING/MONITORING AGENCY REPORT NUMBER

NASA TM-106359

11. SUPPLEMENTARY NOTES

V.M. Radhakrishnan, National Research Council—NASA Senior Research Associate, on leave from Indian Institute of Technology, Department of Metallurgical Engineering, Madras, India; Sreeramesh Kalluri, Sverdrup Technology, Inc., Lewis Research Center Group, 2001 Aerospace Parkway, Brook Park, Ohio 44142 (work funded by NASA Contract NAS3-25266); and Gary R. Halford, NASA Lewis Research Center. Responsible person, Sreeramesh Kalluri, (216) 433-6727.

12a. DISTRIBUTION/AVAILABILITY STATEMENT

Unclassified - Unlimited
Subject Category 39

12b. DISTRIBUTION CODE

13. ABSTRACT (*Maximum 200 words*)

The low cycle fatigue behavior of Haynes 188 and B1900+Hf under isothermal, bithermal, and thermomechanical loading conditions has been analyzed on the basis of the total hysteresis energy expended per cycle. It has been observed that in the case of isothermal fatigue the total hysteresis energy correlates well with the fatigue life. In the case of bithermal "high rate" fatigue, for a given total hysteresis energy per cycle, the fatigue life is equal to or greater than the isothermal fatigue life at the maximum bithermal temperature. This observation could be used to establish a lower bound on life for design purposes. In one case of bithermal creep-fatigue and in thermomechanical fatigue, the life is shorter than that corresponding to the isothermal life at the maximum temperature. The energy supplied, per se, may not always give a systematic correlation with the fatigue life in the cases where time-dependent creep and environmental effects are encountered. Thus, in bithermal creep-fatigue and thermomechanical fatigue, the role of creep and environment and their dependence on the energy supplied have to be properly accounted for before the energy term could be used for life prediction.

14. SUBJECT TERMS

Fatigue (metal); Isothermal fatigue; Bithermal fatigue; Thermomechanical fatigue; Creep-fatigue; Hysteresis loop; Strain energy density; Life prediction

15. NUMBER OF PAGES

25

16. PRICE CODE

A03

17. SECURITY CLASSIFICATION OF REPORT	18. SECURITY CLASSIFICATION OF THIS PAGE	19. SECURITY CLASSIFICATION OF ABSTRACT	20. LIMITATION OF ABSTRACT
Unclassified	Unclassified	Unclassified	